

## Estimation of harmonic interference parameters of surface-NMR signal using an adaptive method and residual signal power

Reza Ghanati<sup>1,2\*</sup> and Mohammad Kazem Hafizi<sup>3</sup>

<sup>1</sup>Assistant Professor, Institute of Geophysics, University of Tehran, Tehran, Iran

<sup>2</sup>Leibniz Institute for Applied Geophysics, Stilleweg 2, 30655 Hannover, Germany

<sup>3</sup>Professor, Institute of Geophysics, University of Tehran, Tehran, Iran

(Received: 18 January 2017, Accepted: 18 October 2018)

### Abstract

Surface nuclear magnetic resonance (surface-NMR) method is a well-known tool for determining the water-bearing layers and subsurface resistivity structure. Harmonic interference is an inevitable interference in surface-NMR measurements. Accurate estimation of harmonic interference parameters (i.e., fundamental frequency, phase and amplitude) leads to better retrieval of power-line harmonics and consequently, more effective suppression of harmonics from surface-NMR recordings. To that end, two algorithms are addressed for isolation and then subtraction of harmonic interfering noise based on modeling of power-line harmonics by a modified version of Nyman-Gaiser estimation (NGE) and residual signal power (RSP) technique. Then, the results derived from the proposed algorithms are analyzed and compared through the modeling of some synthetic signals embedded in simulated noise and real recordings obtained from multi-channel surface-NMR measurements. The numerical experiments on simulated and real surface-NMR signals show that the application of the proposed procedures results in significant decline of the level of the standard deviation of imaginary part of the detected signal and consequently, relatively accurate recovery of the harmonic signal components with an accompanying enhancement in estimation of the surface-NMR signal parameters.

**Keywords:** surface-NMR signal, harmonic interference, parameter estimation, signal power

## 1 Introduction

Contrary to other geophysical tools the surface nuclear magnetic resonance (surface-NMR) method, due to the direct sensitivity to the underground water molecules, provides significant information regarding the distribution of water content in the shallow subsurface and, to a much lesser extent, pore geometry and hydraulic conductivity. Despite the exclusive properties of the surface-NMR method, it is strongly affected by the presence of ambient electromagnetic interferences, i.e., power-line harmonics, so that estimation of the signal parameters prior to the noise removal process may lead to inaccurate calculation of the petro-physical parameters of the aquifer. Surface-NMR, also called magnetic resonance sounding (MRS), energizes the nuclei of the hydrogen atoms of water molecules (i.e. protons) in the subsurface by transmitting a resonance EM pulse, and then the energized protons generate a secondary magnetic resonance signal after the excitation pulse is switched off. The signal response of the hydrogen nuclei which is an exponentially decaying function of time resonates at the proton Larmor frequency with signal phase. As for most geophysical measurements, surface-NMR data are frequently corrupted by various types of noise. It is well-known that the surface-NMR is affected by two environmental electromagnetic noise sources including power-line harmonics and noise spikes. Harmonic interference is complicated by time-varying nature of the fundamental frequency and harmonic content as well as the varying characteristics across different power grids. Harmonic interfering noises have more destructive contribution among other noises presented in surface-NMR measurements. The weakness of the recorded signal causes the measurements to be intensely noise corrupted, and

hence, robust and effective noise attenuation schemes are required in order to preserve the signal of interest, which leads eventually to an increase in the accuracy of the parameter estimation.

Whereas signal processing is an integral part of getting MRS sounding with an acceptable signal to noise ratio, to date, great efforts have been devoted to developing surface-NMR noise attenuation methods in terms of single- and multi-channel systems. For instance, the application of block subtraction, sinusoid subtraction and notch filtering methods to the single-channel data for suppression of power-line harmonics proposed by Legchenko and Valla (2003). They proved that the notch filtering was the most drastic, but it may pervert the signal of interest, and this distortion increases when the signal frequency is close to one of the parasitic harmonics (less than 8 Hz). The advent of multi-channel systems (Walsh, 2008), the second generation of surface-NMR instruments, allows to use advanced processing techniques and it is possible to overcome the defects from the single-channel based surface-NMR filtering methods (see Müller-Petke & Costabel, 2014; Larsen et al., 2014; Costabel and Müller-Petke, 2014; Ghanati et al., 2014, Ghanati and Fallahsafari, 2015). Using the multi-channel measurements, an improvement in estimation of the MRS signal parameter was achieved through Wiener filtering and adaptive noise cancellation (Dalgaard et al., 2012). The results from the study showed that the two procedures provided the same noise cancelling performance.

In this paper, the estimation of harmonic interference parameters of surface-NMR signal is treated using two harmonic noise cancellation methods (i.e., modified Nyman-Gaiser estimation (MNGE) and residual signal power (RSP)) with special emphasis on the cases when one power-line harmonic

frequency is close to the signal frequency (Larmor frequency). It should be noted that the major difference between the proposed methodologies is in the estimation approach of the fundamental frequency so that the better the fundamental frequency estimation, the more accurate the harmonics' retrieval will be. After power-line harmonic interference cancelling, the parameters of the processed signal can be derived by the envelope detection process, including signal extraction using a novel method called digital quadrature detection with additional phase correction (Ghanati et al., 2016b) and the estimate of the surface-NMR signal parameters (i.e., relaxation time  $T_2$ , initial amplitude  $E_0$ , Larmor frequency  $f_L$  and phase  $\phi_0$ ). The rest of the paper is organized as follows: In section 1, the theory of the proposed approaches is developed. The functionalities of the proposed schemes are dealt with through synthetic signal corrupted by noise and a real data set in section 3, and the last section is devoted to some concluding remarks.

## 2 Theory

In what follows, a detailed description of the MNGE and RSP algorithms is presented for understanding the performance of the proposed methods in surface-NMR processing.

### 2.1 Modified Nyman-Gaiser Estimation method

The proposed method is an extended version of Nyman-Gaiser estimation (Nyman and Gaiser, 1983) for suppressing power-line noise in the surface-NMR recordings (Saucier et al., 2006). This technique involves subtracting an estimation of the harmonic component without distorting or enervating the signal of interest. Nyman & Gaiser (1983) demonstrated that it is possible to eliminate harmonic interfering

noise by modeling the noise as a sum of stationary sinusoids and then subtracting them from each trace. Their technique includes finding a refined fundamental frequency and then sequentially finding phase and amplitude for each harmonic component through Fourier analysis of time series.

A recorded surface-NMR signal  $V(t)$  can be represented by the following model:

$$V_n = E_n + P_n + \vartheta_n, \quad (1)$$

where  $E_n$  is the ideal surface-NMR signal from the subsurface protons defined as:

$$E(t) = E_0 \cos(2\pi f_0 t + \phi_0) \exp(-t / T_2^*), \quad (2)$$

where  $E_0$  is the initial amplitude,  $T_2$  denotes decay time of the FID signal and  $f_0$  indicates the Larmor frequency,  $\phi_0$  is the phase offset of the signal, and  $P_n$  is the power-line interference,  $\vartheta_n$  is the non-harmonic noise (i.e., spiky events and Gaussian noise), and  $n$  is the time index.  $P_n$  consists of a set of harmonic sinusoidal components with unknown frequencies, phases and amplitudes as:

$$\begin{aligned} P &= \sum_{k=1}^M C_k \cos(k\omega_0 n + \Theta_k) \\ &= \sum_{k=1}^M P_k \\ &= \sum_{k=1}^M a_k \cos(k\omega_0 n) + b_k \sin(k\omega_0 n), \end{aligned} \quad (3)$$

where  $\omega_0 = 2\pi f_0 / f_s$ ,  $f_0$  and  $f_s$  are the harmonic signal (or fundamental frequency) and sampling frequencies, respectively, and the amplitude and phase of the  $k^{\text{th}}$  harmonic are denoted by  $C_k$  and  $\Theta_k$ , respectively, and  $M$  indicates the number of harmonics presented in the interference. An appropriate harmonic interference elimination algorithm should remove the interference  $P$ , while preserving the free induction decay signal  $E$ . Note that the amplitude, phase and frequency of all harmonics are assumed

to remain constant over the length of the record. This assumption is generally reasonable for record lengths of a few seconds or less (Butler & Russell, 1993; Larsen et al., 2014). Whereas the maximum signal length, which is recorded by the surface-NMR instruments is less than 1 s, the above assumption is accepted as being valid for the surface-NMR measurements (Ghanati et al., 2016b).

The harmonic noise  $P$  given by Equation (3) may also be written in this form:

$$P = \sum_{k=1}^M a_k \cos(k\omega_0 n) + b_k \sin(k\omega_0 n), \quad (4)$$

where  $a_k = C_k \cos(\Theta_k)$  and  $b_k = C_k \sin(\Theta_k)$ . Putting Equation (4) into Equation (3), the following equation will be resulted. Note that the term  $\vartheta$  is neglected for simplicity.

$$V = E + \sum_{k=1}^M a_k \cos(k\omega_0 n) + b_k \sin(k\omega_0 n). \quad (5)$$

The recent equation can be written as a system of linear equation:  $\mathbf{X} = H\mathbf{d} + \mathbf{S}$ , where  $\mathbf{E} = (s_1(t), s_2(t), \dots, s_N(t))^T$ ,  $\mathbf{d} = (a_1, b_1, \dots, a_M, b_M)^T$ ,  $\mathbf{V} = (x_1, x_2, \dots, x_N)^T$ , and  $H$  is an  $N \times 2M$  matrix with  $H_{n,2i-1} = \cos(i\omega_0 n)$ ,  $H_{n,2i} = \sin(i\omega_0 n)$  for  $n = 1, 2, \dots, N$ ,  $i = 1, 2, 3, \dots, 2M$ . If  $E$  is assumed to have Gaussian distribution, the maximum likely estimator of  $V$  is  $H\tilde{\mathbf{d}}$  where  $\tilde{\mathbf{d}}$  is the standard least-squares solution and hence:

$$\begin{aligned} \hat{d} &= \arg \min_{\mathbf{d} \in \mathbb{R}^{2M}} V - H\mathbf{d}^2 \\ &= (\mathbf{H}^T \mathbf{H})^{-1} \mathbf{H}^T \mathbf{s}. \end{aligned} \quad (6)$$

For a certain value of the fundamental frequency  $f_0$ , an estimator  $\tilde{\mathbf{d}}$  of the amplitude  $\mathbf{d}$  can be computed by minimizing the above cost function.

Based on the NGE methodology, frequency  $f_0$  is known to be approximately equal to  $f_n = 50$  Hz to estimate the amplitude and phase. Considering an initial guess  $f_n$  of  $f_0$ , NGE generates an estimate  $\tilde{\delta}$  of the fundamental frequency shift  $\delta$  as:

$$f_0 = f_n + \delta. \quad (7)$$

Once  $\tilde{\delta}$  is achieved, the frequency estimate is revised with  $f_n^{r+1} = f_n^r + \tilde{\delta}$ , where  $r$  is the number of iteration, and this value is used as a starting value for the next iteration. The optimization process is continued until the convergence of  $\tilde{f}$  is achieved. The NGE algorithm estimates each harmonic separately, leading to a collection  $(\tilde{f}_1, \tilde{f}_2, \dots, \tilde{f}_M)$  of harmonic frequency estimates. Whereas these frequencies  $f_n$  are related to each other by  $f_n = n f_0$  ( $n = 1, 2, \dots, M$ ), it is possible to use a linear combination of the estimates  $\tilde{f}_1, \tilde{f}_2, \dots, \tilde{f}_M$  to construct a single lower variance estimator of the fundamental frequency  $f_0$ .

The proposed method is based on the Nyman and Gaiser's estimation variables defined as (discrete form of the corresponding equations):

$$\mathbf{O}_k = (1/N) \sum_{n=1}^{N-1} \cos(k\omega_0 n) V_n, \quad (8a)$$

$$P_k = (1/N) \sum_{n=1}^{N-1} \sin(k\omega_0 n) V_n, \quad (8b)$$

$$Q_k = (1/N) \sum_{n=1}^{N-1} \left( \frac{\cos(k\omega_0 n)}{\sin(\frac{2\pi n \Delta t}{T})} V_n \right), \quad (8c)$$

$$R_k = (1/N) \sum_{n=1}^{N-1} \left( \frac{\sin(k\omega_0 n \Delta t)}{\sin(\frac{2\pi n \Delta t}{T})} V_n \right), \quad (8d)$$

where  $T$  is signal duration and  $k = 1, 2, \dots, M$ . The above estimation variables are used to construct an estimator of the  $k^{\text{th}}$  harmonic. Note that

the amplitude  $C_k$  and phase  $\Theta_k$  of the  $k^{\text{th}}$  harmonic are estimated using the variables  $O_k$  and  $P_k$ , respectively. The variables  $Q_k$  and  $R_k$  allow the estimation of the frequency shift  $\delta = f_0 - f_n$ . Using Equation (8) a collection of  $M$  estimators of  $\tilde{\delta}_k$  of  $\delta$  is expressed as follows:

$$\tilde{\delta}_k = \frac{F_k(O_k, P_k, Q_k, R_k)}{kT(O_k^2 + P_k^2)} = \frac{2\pi(O_k R_k - P_k Q_k)}{kT(O_k^2 + P_k^2)} \quad (9)$$

Equation (9) defines one estimator of  $\delta$  for each harmonic of the fundamental frequency. It can be proved that  $\tilde{\delta}_k$  are unbiased estimators of  $\delta$ .

The estimators of  $\tilde{C}_k$  and  $\tilde{\Theta}_k$  of  $C_k$  and  $\Theta_k$  are also represented by:

$$\tilde{C}_k = 2\sqrt{O_k^2 + P_k^2}, \quad (10a)$$

$$\cos(\tilde{\theta}_k) = \frac{2(O_k - \pi Q_k)}{\tilde{C}_k}, \quad (10b)$$

$$\sin(\tilde{\theta}_k) = -\frac{2(P_k - \pi R_k)}{\tilde{C}_k}. \quad (10c)$$

In the statistical context, an optimum estimator needs to be unbiased; meaning that on the average, the estimator will yield the true value of the unknown parameter, and minimizes the variance criterion (Kay, 1993). Such an estimator is called the minimum variance unbiased (MVU) estimator. The determination of the MVU estimator is in general a difficult task because it often occurs in practice the MVU estimator, if it exists, cannot be found. For instance, nobody may know the probability density function (PDF) of the data or even be willing to assume a model for it. In this case, even some methods that take advantage of the Cramer-Rao lower bound (Kay, 1993), which is a lower bound on the variance of any unbiased estimator, and the theory of sufficient statistics (Fisher, 1922) cannot be

applied. Faced with our inability to determine the optimal MVU estimator, it is reasonable to resort to a suboptimal estimator. However, if the variance of the suboptimal estimator can be ascertained, and if it meets our system properties, then its use may be justified as being adequate for the problem at hand. If its variance is too large, then it is needed to consider other suboptimal estimators to detect one that meets the specifications. A common practice is to limit the estimator to be linear in the data and find the linear estimator that is unbiased and has minimum variance. This estimator is termed the best linear unbiased estimator (BLUE) and can be determined without complete knowledge of the PDF of the data (Kay, 1993).

Saucier et al. (2006) demonstrated that the BLUE can be used to develop a single estimator for the error in the initial estimate of the fundamental frequency. This single estimator combines all the estimates for the frequency shifts  $\tilde{\delta}_k$  and amplitudes for each of the harmonics. Whereas the variables  $\tilde{\delta}_k$  are uncorrelated, which is the consequence of the orthogonality of the estimation variables (Equation (8)), according to Saucier et al. (2006) for mutually uncorrelated variables, the BLUE takes the form as:

$$\tilde{\delta} = \frac{\sum_{k=1}^M \frac{\tilde{\delta}_k}{\sigma_k^2}}{\sum_{k=1}^M \frac{1}{\sigma_k^2}}, \quad (11)$$

where  $\sigma_k^2 = \text{Var}(\tilde{\delta}_k)$  and  $\text{Var}(\tilde{\delta}) = \frac{1}{\sum_{k=1}^M \sigma_k^{-2}}$ . It can be proved that  $\sigma_k^2$  is defined as (the readers are referred to Saucier et al. (2006), for more details about determination of variance of estimation variables):

$$\sigma_k^2 \approx \frac{4\pi^2 \sigma^2}{A_k^2 k^2 T^3}, \quad (12)$$

where  $\sigma^2$  is the white process variance. Substituting the recent equation into Equation (17), the BLUE takes the following form:

$$\tilde{\delta} = \frac{\sum_{k=1}^M \tilde{\delta}_k k^2 \tilde{C}_k^2}{\sum_{k=1}^M \tilde{C}_k^2 k^2}. \quad (13)$$

### 2.1.1 Algorithm implementation

First, the estimation variables for  $k = 1, 2, \dots, M$  are calculated with the discrete form of Equation (8) using the initial angular-frequency estimates  $\omega_k = k2\pi f_n / f_s$ . Then the frequency shifts  $\tilde{\delta}_k$  are determined using Equation (9). The amplitudes is then computed with the help of Equation (10a), and the results are used in Equation (13) to obtain the angular-frequency shift estimate  $\tilde{\delta}$ . Afterwards,  $\tilde{\delta}$  is used to revise the initial angular-frequency estimate with  $\omega_0^{new} = \omega_0 + \tilde{\delta}$ . The optimization process is continued with this new angular-frequency estimate until  $\omega$  converges. Once  $\omega$  is calculated, the amplitude estimation problem is implemented using the cost function given by Equation (6) so that the final amplitudes obtained by using Equation (6) are more accurate than those of Equation (10). Note that the convergence rate associated with the proposed method is relatively faster than the NGE algorithm so that the convergence of the proposed method is usually achieved with less than six iterations. In the following, a deterministic method based on residual signal power are demonstrated.

### 2.2 Residual signal power

The residual signal power method is carried out by modeling the harmonics through the estimation of the harmonic components (i.e., fundamental frequency  $f_0$ , amplitude  $C_k$  and phase  $\Theta_k$ ) (Larsen et al., 2014). The RSP algorithm consists

of two steps where the fitting of  $C_k$  and  $\Theta_k$  is a linear optimization problem, and the fitting of  $f_0$  is a non-linear problem. The fundamental frequency  $f_0$  is determined at the first stage, and at the second stage using  $f_0$  derived from the previous step, the parameters  $C_k$  and  $\Theta_k$  are calculated through Equation (6). In contrast to the MNGE method, in the recent proposed scheme, a search of the optimum fundamental frequency is performed using the modeling of harmonics through frequencies varying with sequential steps around 50 Hz. The modeled harmonics based on the assumed values of the fundamental frequency are subtracted from the recorded signal so that the assumed value of  $f_0$  resulting in the minimum residual power signal is chosen as the true fundamental frequency. After the estimation of the fundamental frequency, the amplitudes and phases associated to each of harmonics are modeled using Equation (6). It should be noted that in RSP all harmonics are removed, except for the harmonic close to the Larmor frequency, on the whole time-series. Then, amplitude and phase of the excluded harmonic are calculated based on fitting the model of the corresponding harmonic, the last 500 ms of the time-series and extrapolating to the first 500 ms. Subsequently, the model parameters of the harmonic adjacent to the Larmor frequency are estimated using the last part of the FID signal where the MRS signal is vanishingly small. Figure 1 illustrates the residual signal power associated to an assumed range of fundamental frequency  $f_0$  between 49.8 Hz and 50.8 Hz after modeling of a synthetic surface-NMR corrupted by a real noise recording and removal of parasitic harmonics. It can be seen that choosing fundamental frequency equal to 50.03 gives best removal of harmonic components. Furthermore, the minimum RSP can be determined to within roughly

1 mHz, and deviation of the estimated fundamental frequency of just a few mHz from the optimum value will affect the noise cancelling efficiency of the RSP algorithm.

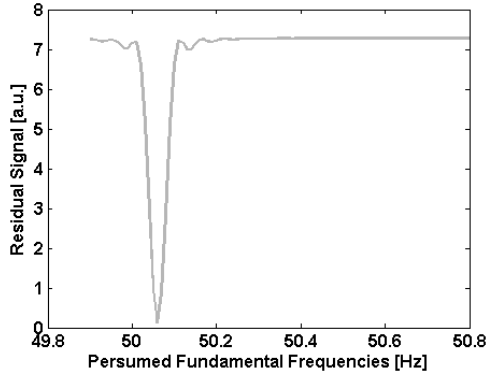


**Figure 1.** Representation of the residual signal power after modeling and cancellation of harmonics at the resumed fundamental frequencies. Choosing fundamental frequency equal to 50.03 gives minimum residual signal power, and consequently, best removal of harmonic components.

### 3 Numerical experiments

In this section, the proposed filtering algorithms are applied to synthetic surface-NMR signal contaminated with simulated noise and real surface-NMR signal. Two metrics in terms of signal-to-noise ratio improvement and mean absolute percentage error (MAPE) are used to quantify the quality of the retrieved signal. Mathematically, MAPE is expressed as:

$$\text{MAPE} = \frac{1}{N} \sum_{i=1}^N \left| 100 \times \frac{S(t_i) - \hat{S}(t_i)}{S(t_i)} \right|, \quad (14)$$

where  $\hat{S}(t_i)$  is the reconstructed signal (the processed and stacked signal), and  $S(t_i)$  is the ideal signal.

It should be noted that after filtering and before estimation of the signal parameters, signal detection is carried out using the digital quadrature detection with phase correction (DQDp) to extract the surface-NMR signal envelope. The

DQDp process is implemented through the following four stages:

1) Multiplication of the FID signal  $S(t)$  by  $e^{(-j2\pi f_R t)}$

2) The phase correction done by multiplying the complex signal, obtained from the previous step, with  $e^{(-j\alpha)}$

3) Implementation of a low-pass filter for further enhancement of the signal-to-noise ratio.

Here,  $f_R$  denotes the frequency of the excitation signal and  $\alpha$  is the phase offset of the signal defined as (see Appendix A for more details):

$$\alpha = \tan^{-1} \left( \frac{\sum_{n=1}^N \text{imag}(S(t)e^{(-j2\pi f_R t)})}{\sum_{n=1}^N \text{real}(S(t)e^{(-j2\pi f_R t)})} \right). \quad (15)$$

The application of the DQDp scheme leads to two signals, one in phase (real part) and one in out-of-phase (imaginary part) where the real part of the signal is composed of noise and the FID, while the imaginary part includes only noise components (Neyer, 2010; Müller-Petke et al., 2011). Hence, the real part is used for mono-exponential fitting. Note that after signal detection, the imaginary part merely contains noise, and thus, it (standard deviation of the imaginary part), as will be shown later, is used to measure the noise level of the processed signal (i.e., real part). In general, decreasing the standard deviation of the imaginary part means a better removal of power-line harmonics. Subsequently, in order to estimate the signal parameters including initial amplitude, signal frequency, phase, and relaxation time, a non-linear inverse problem based on the regularized Levenberg–Marquardt method (Chavent, 2009) is used.

#### 3.1 Application to simulated surface-NMR signal

In this subsection, the performance of the proposed harmonic mitigation methods

are tested using synthetic modeling with known parameters. Two surface-NMR signals are simulated through Equation (2) with the parameters defined in Table 1. Then, the corresponding signals are corrupted by Gaussian noise with a standard deviation of 110 nV and zero mean and harmonic signals with frequencies starting at 1800 to 2250 Hz and the amplitude of each harmonic is randomly chosen between 120 nV and 200 nV. The numerical procedure is repeated 20 times to generate both the first signal and the second signal. Figures 2(a) and (b) show the resulting simulated signals for one single record associated to signal 1 and signal 2, respectively. Furthermore, the power spectral density (PSD) of noise free (green curve) and noise added (grey curve) signals 1 and 2 is plotted in Figures 2(c) and (d), respectively. Referring to Figure 2, it can be observed that the surface-NMR signals are completely masked by electromagnetic noise and consequently the decaying exponential form is not observable, as well as the Larmor frequencies associated to signals 1 and 2 appear close to one of the harmonics, which makes noise cancellation more difficult, particularly for signal 1. As mentioned earlier, the difference between MNGE and RSP is in estimation of the fundamental frequency so that the process of optimum selection of the fundamental frequency in MNGE and RSP is carried out using a statistical optimization problem and non-linear problem, respectively. The envelopes of the resulting signals obtained from the proposed filtering algorithms and merely use of pure stacking in the time and frequency domains are shown in Figure 3 where after the application of the

algorithms, the harmonic signals are adequately suppressed and the decaying exponential form is easily observable. From Figures 3(e) and (f), it is also seen that merely using of pure stacking fail to adequately eliminate the harmonics while the application of the MNGE and RSP schemes leads to significant removal of harmonic signals. Likewise, representative results from the proposed filtering strategies (i.e., pure stacking, MNGE and RSP) to retrieve the MRS signal parameters are shown in Table 2. It is noteworthy that the efficiency of the proposed filtering schemes is determined using the level of the standard deviation of the imaginary part of the detected signal containing merely noise. With reference to Table 2 it is seen that after the implementation of the proposed algorithms, the values of standard deviation of the processed signals highly decreases, and a close agreement is found between the estimated and assumed model parameters. One can also see that the difference between the results obtained using the RSP method and that of MNGE is trivial in terms of the values of MAPE and standard deviation. Note that the standard deviation of the estimated signal parameters are derived from 10 independent runs of signal creations.

**Table 1.** Assumed parameters for synthetic signals 1 and 2 contaminated with simulated noise signals.

Signals	Signal 1	Signal 2
<b>Parameters</b>		
$E_0$ (nV)	160	170
$T_2$ (ms)	120	110
$f_0$ (Hz)	1905	1910
$\phi_0$ (rad)	1	1.2

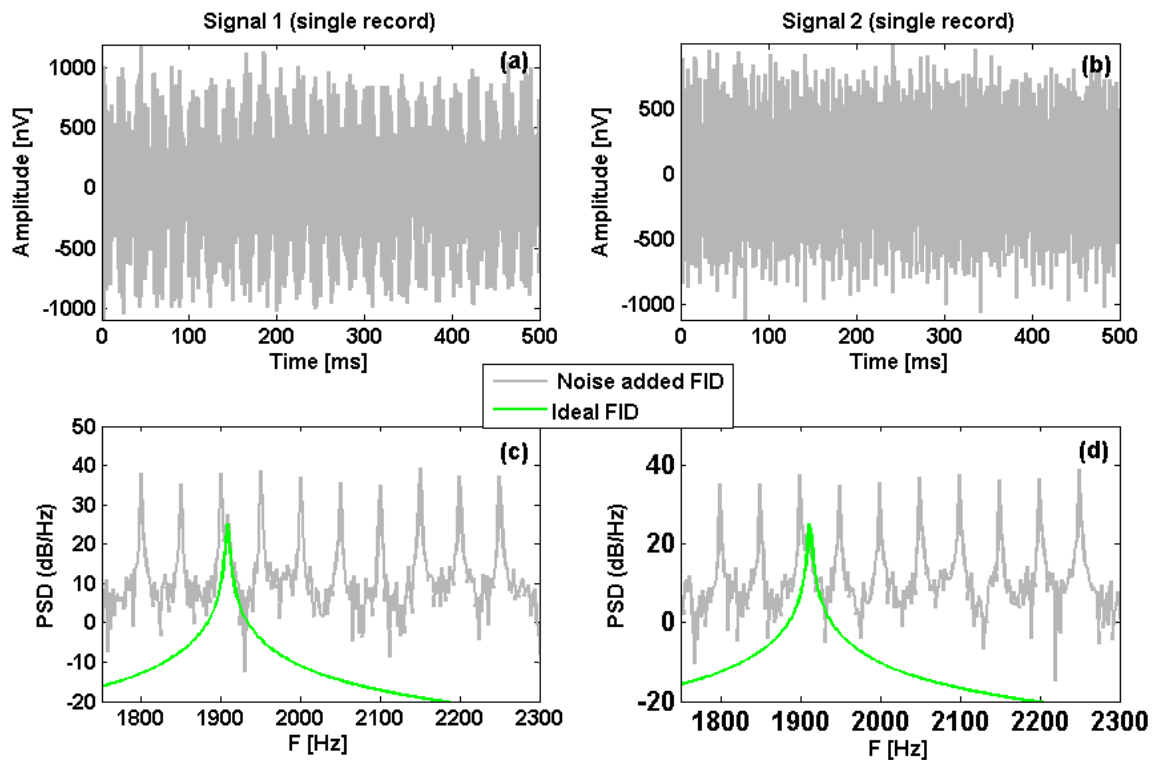


**Figure 2.** Simulated noise-added signals 1 and 2 in the time (top panels) and frequency (bottom panels) domains along with noise free signal in the frequency domain.

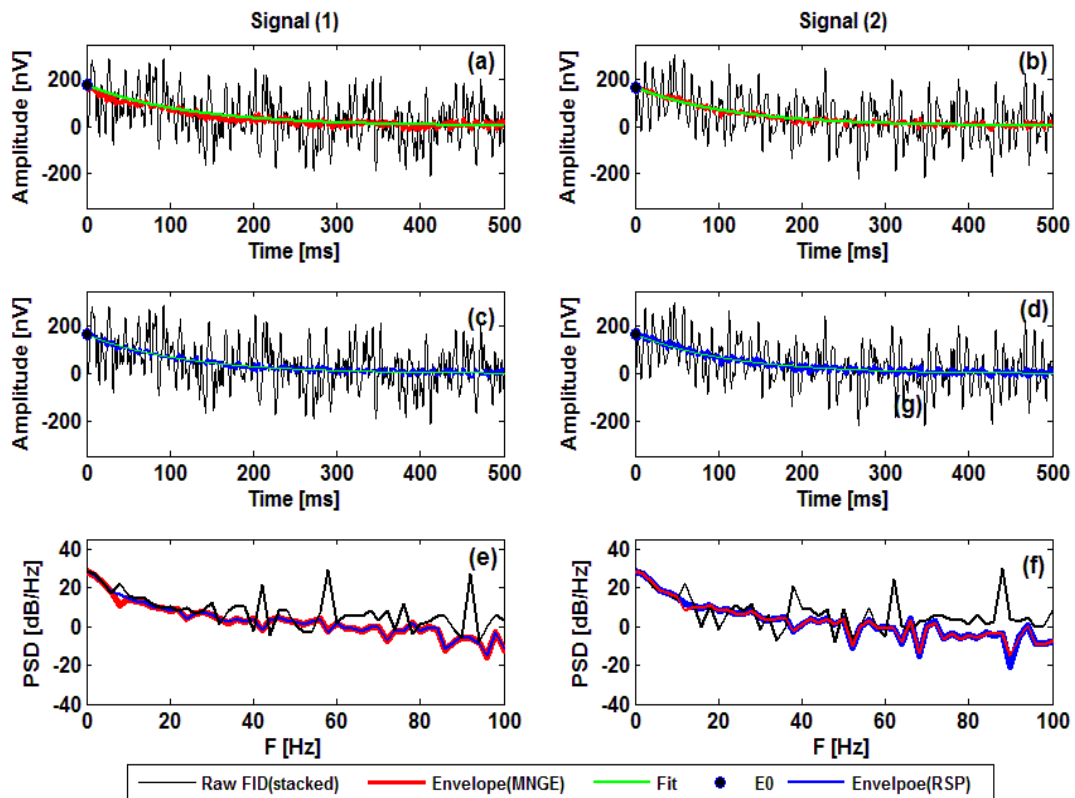


**Figure 3.** Results of signal detection process after applying different noise cancellation strategies to signal 1 (left column) and signal 2 (right column) corrupted by simulated noises. Green line, exponential decay curve defined by the fit-parameters  $T_2$  and  $E_0$  obtained from MNGE (red curve) and RSP (blue curve)-based filtering; dot, initial amplitude of the estimated signal.

**Table 2.** Performance comparison results of MNGE and residual signal power methods implemented on signals 1 and 2 with initial amplitudes  $E_0 = 160$  and  $170$  nV, relaxation times  $T_2 = 120$  and  $110$  ms, phase  $\phi_0 = 1$  and  $1.1$  rad, and the Larmor frequencies equal to  $1905$  and  $1910$  Hz, respectively. The resulting signal parameters are computed from 10 independent runs.

Methods Parameters	Signal 1			Signal2		
	Pure stacking	MNGE <sup>a</sup>	RSP <sup>b</sup>	Pure stacking	MNGE	RSP
$E_0$ (nV)	171.58±9.89	157.96±2.87	163.37±4.06	163.37±4.06	170.71±3.07	171.73±1.29
$T_2$ (ms)	129.19±11.24	121.83±2.5	118.15±2.65	118.15±2.65	113.23±2.6	109.29±2.12
$f_0$ (Hz)	1904.91±0.07	1906.01±0.03	1904.97±0.06	1904.97±0.06	1910.04±0.01	1909.96±0.023
$\phi_0$ (rad)	0.94	1.02	0.986	0.986	1.13	1.108
STD <sup>c</sup>	39.03±6.16	4.48±0.5	3.99±0.58	3.99±0.58	5.026±0.7	4.60±1.87
MAPE <sup>d</sup> [%]	17.82±2.11	4.25±2.16	3.34±2.22	3.34±2.22	7.28±3.2	3.25±2.03

<sup>a</sup> MAPE: Mean Absolute Percentage Error, <sup>a</sup> Modified Nyman-Gaiser estimation, <sup>b</sup> Residual Signal Power, <sup>c</sup> Standard Deviation (associated to imaginary part of signal envelope).

### 3.2 Application to real data

In the previous subsection, a performance comparison of the proposed noise cancellation algorithms was demonstrated by presenting the results of implementing MNGE, RSP and pure stacking on two synthetically corrupted MRS records where promising results were shown in terms of reduction of the level of the standard deviation of the detected signal, and reasonable retrieval of the model parameters. In the following, the efficiency of the corresponding strategies is tested using a real surface-NMR record. Surface-NMR field measurements were carried out through the NUMIS<sup>POLY</sup> apparatus from Iris Instruments with sampling frequency of  $19200$  Hz and using a  $100$  m-diameter-circle loop with one turn. An example of the recorded surface-NMR signal in the time and frequency domains is represented in Figures 4(a) and (b), respectively. It is evident that the power spectrum is dominated by the power-line harmonics at multiples of  $50$  Hz. Surface-NMR is usually contaminated by electrical discharges from both natural and artificial sources bringing about spiky events so that prior to implementing harmonic noise cancellation methods, spiky noises are suppressed from surface-NMR measurements. However, after harmonic cancelation, often a number of small spikes that were masked by the harmonic

noises appear so that a second spike removal process is implemented. Furthermore, to improve the performance of the proposed algorithms, a band-pass of  $150$  Hz bandwidth is applied prior to the implementation of MNGE and RSP. It should be noted that choosing improper bandwidth of the band-pass filter may yield the elimination of a large part of the signal energy (Ghanati et al., 2016b). The envelope detected after processing by using MNGE (red curve) and RSP (blue curve) are displayed in Figures 4(c) and (d), respectively. Moreover, the resulting signals after de-noising in the frequency domain are depicted in Figure 4(e). Referring to Figure 4(e), the harmonic components seen in the original surface-NMR signals are no longer observed in the processed signal through the proposed filtering methods, and the Larmor frequency remain unchanged while merely use of the stacking process fails to adequately eliminate power-line harmonics. In addition, the estimated parameters of the surface-NMR signal are provided in Table 3. As seen through the proposed harmonic cancellation strategies the level of the standard deviation of the imaginary part of the detected signals is considerably reduced compared to merely use of stacking process. In addition, a relatively close correlation can be seen between the estimated parameters using the MNGE and RSP methods.

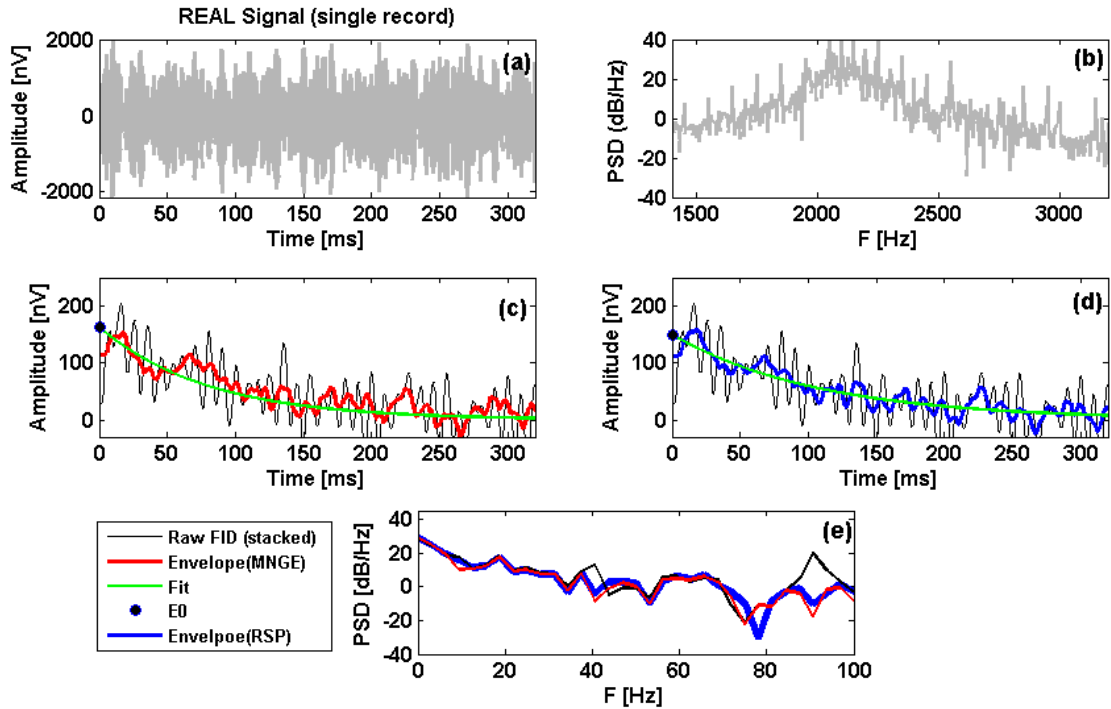


**Figure 4.** At the top: Representation of a real single-record surface-NMR signal in a) the time and b) frequency domains recorded in an area with harmonic interferences. At the bottom: Results of signal detection process in the time domain after applying: c) MNGE (red curve) and d) RSP (blue curve) with pure stacking (black curve) to real surface-NMR record and in the frequency domain, (e). Green line; exponential decay curve defined by the fit-parameters  $T_2$  and  $E_0$  obtained from MNGE- and RSP-based filtering; dot, initial amplitude of the estimated signal.

**Table 3.** Performance comparison results of MNGE and residual signal power methods implemented on real surface-NMR record.

Methods Parameters	Pure stacking	MNGE <sup>a</sup>	RSP <sup>b</sup>
$E_0$ (nV)	173.9	158.37	152.35
$T_2$ (ms)	76.65	89.29	98.51
$f_0$ (Hz)	2141.12	2141.034	2140.97
STD <sup>c</sup>	98.91	7.54	7.69

<sup>a</sup> MAPE: Mean Absolute Percentage Error, <sup>a</sup> Modified Nyman-Gaiser estimation, <sup>b</sup> Residual Signal Power, <sup>c</sup> Standard Deviation (associated to imaginary part of signal envelope).

## 4 Conclusions

The objective of this study was to present two efficient power-line harmonic noise cancellation techniques based on the modified version of Nyman-Gaiser estimation and residual signal power method. The process of retrieval of the parameters of harmonic signals is carried out in two stages: the fundamental frequency is first calculated using a statistical optimization method and signal

power in MNGE and RSP, respectively. At the second stage, amplitudes and phases are calculated using a linear inverse problem in both the MNGE and RSP procedures. The numerical examples showed that the fundamental frequency estimation using either MNGE or RSP results in a reasonable agreement between the assumed frequency and that of MNGE and RSP. Furthermore, the application of the proposed algorithms to synthetic surface-NMR signal embedded in simulated noises and a real surface-NMR record led to remarkable reduction of the standard deviation of the imaginary part obtained from the signal detection process and consequently better estimation of the signal parameters. Besides, digital quadrature detection was used with phase correction, which benefits from the advantage of the signal frequency sensitivity to extract the envelope of the FID signal. Note that the

estimation of the fundamental frequency, due to the deviation in the fundamental frequency generated by power-line generation facilities on the order of 0.03 Hz in industrial countries and 1 Hz in developing countries is still a challenging task.

## References

- Butler, K. E., and Russell, R. D., 1993, Subtraction of power-line harmonics from geophysics records: *Geophysics*, **58**, 898–903.
- Chavent, G., 2009, Nonlinear least squares for inverse problems, *Scientific Computation: Theoretical foundations and step-by-step guide for applications*: Springer, New York.
- Costabel, S., and Müller-Petke, M., 2014, Despiking of magnetic resonance signals in time and wavelet domain: *Near Surface Geophysics*, **12**, 185 – 197.
- Dalgaard, E., Auken, E., and Larsen, J., 2012, Adaptive noise cancelling of multichannel magnetic resonance sounding signals: *Geophysical Journal International*, **191**, 88–100.
- Fisher, R. A., 1922, On the mathematical foundations of theoretical statistics: *Philosophical Transactions of the Royal Society, A*, **222**, 309–368.
- Ghanati, R., Fallahsafari, M., and Hafizi, M. K., 2014, Joint application of a statistical optimization process and Empirical Mode Decomposition to Magnetic Resonance Sounding Noise Cancellation: *Journal of Applied Geophysics*, **111**, 110-120.
- Ghanati, R., Fallahsafari, M., 2015, Comment on: 'Time-based noise removal from magnetic resonance sounding signals' by M. Shahi, H. Khaloozadeh and M. K. Hafizi: *International journal of innovative computing, information and control*, **11**(1), 387–390.
- Ghanati, R., Hafizi, M. K., and Fallahsafari, M., 2016a, Surface nuclear magnetic resonance signals recovery by integration of a non-linear decomposition method with statistical analysis: *Geophysical Prospecting*, **64**, 489–504.
- Ghanati, R., Hafizi, M. K., Mahmoudvand, R., and Fallahsafari, M., 2016b, Filtering and parameter estimation of surface-NMR data using singular spectrum analysis: *Journal of Applied Geophysics*, **130**, 118-130.
- Kay, S. M., 1993, *Fundamentals of statistical signal processing, Estimation theory*: Prentice-Hall.
- Larsen, J. J., Dalgaard, E., and Auken, E., 2014, model-based removal of power-line harmonics and multi-channel Wiener filtering: *Geophysical Journal International*, **196**, 2, 828-836.
- Legchenko, A., and Valla, P., 2003, Removal of power-line harmonics from proton magnetic resonance measurements: *Journal of Applied Geophysics*, **53**, 103-120.
- Müller-Petke, M., and Costabel, S., 2014, Comparison and optimal parameter setting of reference-based harmonic noise cancellation in time and frequency domain for surface-NMR: *Near Surface Geophysics*, **12**, 199 – 210.
- Müller-Petke, M., Dlugosch, R., and Yaramanci, U., 2011, Evaluation of surface nuclear magnetic resonance-estimated subsurface water content: *New Journal of Physics*, **13**.
- Neyer, F. M., 2010, Processing of full time series, multichannel surface-NMR signals: M. Sc. thesis, ETH Zurich.
- Nyman, D. C., and Gaiser, J. E., 1983, Adaptive rejection of high-line contamination: 53rd Annual International Meeting, SEG, Expanded Abstracts, 321–323.
- Saucier, A., Marchant, M., and Chouteau, M., 2006, A fast and accurate frequency estimation method for canceling harmonic noise in geophysical records: *Geophysics*, **71**, V7-V18.
- Walsh, D. O., 2008, Multi-channel surface NMR instrumentation and soft-ware for 1D/2D groundwater investigations: *Journal of Applied Geophysics*, **66**, 140–150.

## Appendix

### Signal detection using digital quadrature method

The procedure described here detects the surface-NMR signal using digital quadrature detection with phase correction.

Considering the surface-NMR signal as follows:

$$V(t, q) = V_0(q) \exp(-t / T_2^*) \cos(2\pi f_L t + \theta(q)). \quad (A1)$$

Multiplication of  $V(t, q)$  by  $\exp(-j2\pi f_R t)$  gives:

$$V_c(t) = V(t) \times \exp(-j2\pi f_R t), \quad (A2)$$

and

$$V_c(t) = V_0 \left[ \cos(2\pi f_L t + \theta) \right. \\ \left. \exp\left(\frac{-t}{T_2^*}\right) \exp(-j2\pi f_R t) \right]. \quad (\text{A3})$$

using Euler's formula, we have

$$V_c(t) = V_0 \left[ \frac{e^{j(2\pi f_L t + \theta)} + e^{-j(2\pi f_L t + \theta)}}{2} \right] \\ \exp\left(\frac{-t}{T_2^*}\right) \exp(-j2\pi f_R t), \quad (\text{A4})$$

then

$$V_c(t) = \frac{1}{2} V_0 \left[ \frac{e^{j(2\pi f_L t - 2\pi f_R t + \theta)} + e^{-j(2\pi f_L t + 2\pi f_R t + \theta)}}{2} \right] \exp\left(\frac{-t}{T_2^*}\right). \quad (\text{A5})$$

By applying a low-pass filter on  $V_c(t)$ , we get

$$V_c(t) = \frac{1}{2} V_0 \left[ e^{j(2\pi f_L t - 2\pi f_R t + \theta)} \right] \exp\left(\frac{-t}{T_2^*}\right), \quad (\text{A6})$$

and

$$V_c(t) = \frac{1}{2} V_0 \left[ \frac{\cos(2\pi(f_L - f_R)t + \theta) + j \sin(2\pi(f_L - f_R)t + \theta)}{2} \right] \\ \exp\left(\frac{-t}{T_2^*}\right). \quad (\text{A7})$$

The Phase correction is implemented using multiplication of  $V_c(t)$  by  $\exp(-j\varphi)$

$$V_c' = V_c(t) \exp(-j\varphi), \quad (\text{A8})$$

$$\varphi = \tan^{-1} \left( \frac{\sum_{n=1}^N \text{imag}(V(t) e^{-j2\pi f_R t})}{\sum_{n=1}^N \text{real}(V(t) e^{-j2\pi f_R t})} \right), \quad (\text{A9})$$

$$V_c' = \frac{1}{2} V_0 \left[ \frac{\cos(2\pi(f_L - f_R)t + \theta) + j \sin(2\pi(f_L - f_R)t + \theta)}{2} \right] \\ \exp\left(\frac{-t}{T_2^*}\right) \exp(-j\varphi), \quad (\text{A10})$$

$$\exp(-j\varphi) = [\cos(\varphi) - j \sin(\varphi)], \\ \delta f = f_L - f_R.$$

$$V_c' = \frac{1}{2} V_0 \left[ \frac{\cos(2\pi\delta f t + \theta) + j \sin(2\pi\delta f t + \theta)}{2} \right] \\ \exp\left(\frac{-t}{T_2^*}\right) [\cos(\varphi) - j \sin(\varphi)], \quad (\text{A11})$$

$$V_c' = \frac{1}{2} V_0 \left[ \frac{\cos(2\pi\delta f t + \theta) \cos(\varphi) - j \cos(2\pi\delta f t + \theta) \sin(\varphi) + j \sin(2\pi\delta f t + \theta) \cos(\varphi) + \sin(2\pi\delta f t + \theta) \sin(\varphi)}{2} \right] \\ \exp\left(\frac{-t}{T_2^*}\right), \quad (\text{A12})$$

$$V_c' = \frac{1}{2} V_0 \left[ \frac{\cos(2\pi\delta f t + (\theta - \varphi)) + j \sin(2\pi\delta f t + (\theta - \varphi))}{2} \right] \\ \exp\left(\frac{-t}{T_2^*}\right). \quad (\text{A13})$$

The final quadrature detection envelope is obtained by:

$$V_{\text{detected}} = 2 \times \text{real}(V_c'). \quad (\text{A14})$$